Inorganica Chimica Acta 435 (2015) 178–186

Contents lists available at ScienceDirect

Inorganica Chimica Acta

journal homepage: www.elsevier.com/locate/ica

Supramolecular interactions through lone pair(lp)–π and hydrogen bonding in cobalt(III) and manganese(II) derivatives of *N*,*N*′-dimethylvioluric acid: A combined experimental and theoretical study

Rupak Banik [a,1], Subhadip Roy [a,1], Antonio Bauza [b], Antonio Frontera [b,*], Antonio Rodríguez-Diéguez [c], Juan M. Salas [c], Alexander M. Kirillov [d], Shubhamoy Chowdhury [e], Saroj Kr. Das [a], Subrata Das [f,*]

[a] Department of Chemistry, National Institute of Technology (NIT) Agartala, 799 046 Tripura, India
[b] Departament de Quimica, Universitat de les Illes Balears, Crta. de Valldemossa km 7.5, 07122 Palma de Mallorca (Baleares), Spain
[c] Departamento de Quimica Inorganica, Facultad de Ciencias, Universidad de Granada, 18071 Granada, Spain
[d] Centro de Química Estrutural, Complexo I, Instituto Superior Técnico, Universidade de Lisboa, Av. Rovisco Pais, 1049-001 Lisbon, Portugal
[e] Department of Chemistry, Tripura University, Suryamaninagar, 799 022 Tripura, India
[f] Department of Chemistry, National Institute of Technology (NIT) Patna, Ashok Rajpath, Patna 800 005, Bihar, India

ARTICLE INFO

Article history:
Received 30 April 2015
Received in revised form 23 June 2015
Accepted 25 June 2015
Available online 2 July 2015

Keywords:
Cobalt(III)
Manganese(II)
Structure elucidation
Noncovalent interactions
DFT calculations

ABSTRACT

The reactivities of cobalt(II) and manganese(II) salts toward HDMV (*N*,*N*′-dimethylvioluric acid monohydrate) were studied. Reaction of cobalt(II) chloride hexahydrate with HDMV in water–methanol medium at pH = 8.0 led to the formation of a cobalt(III) complex $[Co^{III}(DMV)_3]\cdot 0.5H_2O$ (**1**), whereas the interaction of manganese(II) chloride tetrahydrate with HDMV under similar reaction conditions afforded $[Mn^{II}(H_2O)_6](DMV)_2$ (**2**). Dimethylviolurate anion behaves as a bidentate ligand in **1** and counteranion in **2**. Both compounds were characterized by single-crystal X-ray diffraction, elemental analysis, IR spectroscopy, cyclic voltammetry and thermogravimetric analysis. Presence of Co(III) in **1** indicates the aerial oxidation of the cobalt(II) precursor. In **1**, Co(III) adopts a distorted octahedral $[CoN_3O_3]$ coordination environment through bonding to the three dimethylviolurato anions. In **2**, the $[Mn(H_2O)_6]^{2+}$ cations and $(DMV)^-$ anions are assembled by multiple hydrogen bonds into a complex 3D H-bonded network. It was analyzed from the topological viewpoint, disclosing a binodal 4,8-connected underlying net with the **flu** (fluorite) topology. Electrochemical studies reveal that the compounds undergo a quasi-reversible one electron metal centered redox process. DFT studies were carried out to analyze the supramolecular assemblies in the solid state structures, especially lone pair(lp)–π interactions in **1** and H-bonding network in **2**.

1. Introduction

Complex molecular assemblies and supramolecular arrays constructed from small and relatively simple building blocks are ubiquitous in the natural world. While the intricacies of nature's design are not yet completely understood by us, it is well established that nature utilizes three distinct processes [1] namely, self-assembly [2], self-organization [3], and self-replication [4]. Naturally occurring organic building blocks have specific functionalities in configurations that allow them to interact in a deliberate manner [5]. Protein folding, nucleic acid assembly and tertiary structure, formation of phospholipid membranes, ribosomes and microtubules are notable examples of how nature uses self-assembly which is pivotal for living organisms [5]. The common feature of all biological self-assembly processes is the ability of taking the advantage of numerous weak, noncovalent interactions such as hydrogen bonding, charge-charge, donor–acceptor, π-stacking, van der Waals, hydrophilic and hydrophobic, etc [5]. It is, therefore, of fundamental interest to understand and determine the strengths and directional propensities of such 'weak interactions'.

Supramolecular chemistry studies the interactions between, rather than within, molecules – in other words, chemistry that uses molecules rather than atoms as building blocks [6]. Barbituric acid and its derivatives are useful building blocks for the construction of metal supramolecular/coordination frameworks and organo-inorganic hybrid solids [7]. Violuric acid (H_3Vi) and *N*,*N*′-dimethylvioluric acid (Scheme 1) are derivatives of barbituric acid

* Corresponding authors. Tel.: +91 7677417481 (S. Das).
E-mail addresses: toni.frontera@uib.es (A. Frontera), subrataorgchem@gmail.com (S. Das).
[1] R. Banik and S. Roy contributed equally to this work.

http://dx.doi.org/10.1016/j.ica.2015.06.018
0020-1693/

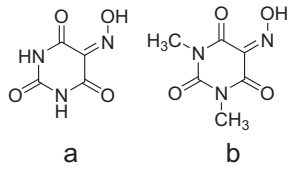

Scheme 1. a = Violuric acid, b = *N*,*N*′-dimethylvioluric acid.

containing C=N—OH substituent at the 5-position on the barbiturate ring. This substituent can provide an extra coordination site compared with barbituric acid itself [8], thus potentially affecting the type of the resulting structures. In addition to metal binding properties, the availability of several hydrogen bond donor and acceptor sites together with the presence of a pyrimidine ring that favors π-stacking interactions, make these molecules very interesting building blocks in context of supramolecular chemistry. Furthermore, there is a considerable number and diversity of applications of violurato derivatives, namely, in analytical chemistry (determination and identification of metal cations) [9], as potent bioactive molecules (antibacterial, antifungal, antihypoxic, antiproliferative and antitumor agents) [10] and redox mediators (e.g., in enzyme-catalyzed degradation of organic pollutants in the industrial effluents and bleaching treatment) [11]. Although various metal complexes of violuric acid [12–18] and *N*,*N*′-dimethylvioluric acid [19–24] have been reported, the investigation of energetic features of supramolecular assemblies observed in such structures has not been undertaken in detail. Very recently, some of our group have reported the structures of *N*,*N*′-dimethylvioluric acid monohydrate and two cadmium(II) complexes obtained from reactions involving HDMV and different *N*-donor ligands (benzimidazole and pyridine) [25]. The compounds presented interesting assemblies in the solid state dominated by hydrogen bonding, π–π and lp–π interactions. Crystal structures of cobalt complexes containing violurate as a ligand, $[Co^{II}(H_2Vi)_2(H_2O)_2]\cdot 2H_2O$ [26] and $[Co^{III}(H_2Vi)_3]\cdot 6H_2O$ [27], have been reported previously. Although a dimethylvioluric acid derivative $[Co^{III}(DMV)_3]$ is known [28], its crystal structure has not been determined earlier. Bearing these points in mind and following our interest in the investigation of supramolecular features in different coordination compounds derived from HDMV, we report herein the preparation, crystal structures, thermogravimetric analysis, electrochemical behavior and DFT studies of two compounds with the formulae of $[Co^{III}(DMV)_3]\cdot 0.5H_2O$ (**1**) and $[Mn^{II}(H_2O)_6](DMV)_2$ (**2**).

2. Experimental

2.1. General remarks and physical measurements

2.1.1. Materials

All chemicals and solvents were obtained from commercial sources and used as received. The synthetic reactions and work-up were done in the open air. HDMV (*N*,*N*′-dimethylvioluric acid monohydrate) was prepared according to a previously described method [20] by means of acid hydrolysis of 6-amino-1,3-dimethyl-5-nitroso uracil with HCl, followed by recrystallization in hot water.

2.1.2. Physical measurements

Elemental analyses (carbon, hydrogen and nitrogen) were performed on a Perkin Elmer CHN analyzer (2400 series II). Infrared (IR) spectra were recorded as KBr disks using a Perkin-Elmer Spectrum 100 FT-IR spectrometer. Thermal behaviors were examined with a Shimadzu TG 50 thermogravimetric analyzer with a heating rate of 10 °C min^{-1} under nitrogen atmosphere. A digital PHB-8 pH meter was used for pH measurements. Magnetic susceptibility measurements were carried out with a Sherwood Scientific Co., UK magnetic susceptibility balance, and diamagnetic corrections were made using Pascal's constants. Cyclic voltammetric (CV) data were acquired on a Bioanalytical Systems Inc. Epsilon electrochemical workstation (Model: CV-50) on a C3 cell stand at 293 K. Dry and degassed solution of **1** and **2**, each of which contained ~1.0 mM of analyte and 0.1 M tetra-n-butylammonium perchlorate (TBAP) as supporting electrolyte, were saturated with nitrogen for 10 min prior to each acquisition. A blanket of nitrogen gas was maintained throughout the measurements. The measurements were carried out with a three-electrode assembly comprising of a Glassy Carbon (GC) working electrode, a platinum wire counter electrode and a Ag/AgCl reference electrode. All potentials reported herein are referenced to Ag/AgCl.

2.2. Synthesis of the complexes

2.2.1. $[Co(DMV)_3]\cdot 0.5H_2O$ (**1**)

A methanol solution (15 ml) of *N*,*N*′-dimethylvioluric acid monohydrate (0.203 g, 1.00 mmol) was added dropwise to an aqueous solution (10 ml) of $CoCl_2\cdot 6H_2O$ (0.120 g, 0.5 mmol) with stirring. The pH of the resulting solution was adjusted to 8.0. The mixture was stirred further for a period of 5 h. The resulting olive-green solution obtained initially changed to orange-red over time. The orange-red precipitate was filtered and the filtrate was allowed to evaporate slowly at room temperature. Diffraction quality red crystals of **1** were obtained from the filtrate after ca. 2 weeks. Yield: 57% based on Co. Elemental *Anal.* Calc. for $C_{18}H_{19}CoN_9O_{12.5}$: C, 34.85; H, 3.09; N, 20.32. Found: C, 34.80; H, 3.07; N, 20.44%. IR (cm^{-1}): 1479 ν(N=O), 1636 ν(C=O), 1682 ν(C=O), 1733 ν(C=O), 3465 $\nu(H_2O)$.

2.2.2. $[Mn(H_2O)_6](DMV)_2$ (**2**)

Compound **2** was synthesized in a similar manner as described for **1**. A methanol solution (15 ml) of *N*,*N*′-dimethylvioluric acid monohydrate (0.203 g, 1.00 mmol) was added dropwise to an aqueous solution (10 ml) of $MnCl_2\cdot 4H_2O$ (0.125 g, 0.5 mmol) with stirring. The solution was adjusted to pH = 8.0 and the stirring was allowed to continue for another 5 h. The resulting pink solution was filtered to remove any small solid particles and allowed to evaporate. Pink block crystals of **2** suitable for X-ray structure determination were collected by filtration after ca. 2.5 weeks. Yield: 44% based on Mn. Elemental *Anal.* Calc. for $C_{12}H_{24}MnN_6O_{14}$: C, 27.13; H, 4.55; N, 15.82. Found: C, 26.95; H, 4.62; N, 15.44%. IR (cm^{-1}): 633 $\rho_w(H_2O)$, 778 $\rho_w(H_2O)$, 1288 ν(C–O), 1481 ν(N=O), 1619 ν(C=O), 1678 ν(C=O), 3414 $\nu(H_2O)$, 3487 $\nu(H_2O)$.

2.3. X-ray data collection and structure refinement

Diffraction data for **1** and **2** were collected at 296(2) K on a Bruker SMART CCD area-detector diffractometer using graphite monochromated Mo Kα radiation (λ = 0.71073 Å). Intensity data were reduced using SAINT [29] and absorption correction was performed by multi-scan method implemented in SADABS [30]. The structures were solved by Charge Flipping using the olex2.solve [31] structure solution program and refined by Least Squares using version 2013-2 of SHELXL [32]. All non-hydrogen atoms were refined anisotropically. Hydrogen atom positions were calculated geometrically and refined using the riding model. There is half a water molecule present in **1** disordered over two positions with equal (0.25) site occupancy factors. A summary of the crystallographic data and structure determination parameters for **1** and **2** is given in Table 1. Selected bond distances and angles for these compounds are listed in Tables 2 and 3. Hydrogen bonding parameters

Table 1
Crystallographic data and structure refinement for **1** and **2**.

Empirical formula	$C_{18}H_{19}CoN_9O_{12.5}$ (**1**)	$C_{12}H_{24}MnN_6O_{14}$ (**2**)
Formula weight	620.35	531.31
T (K)	296(2)	296(2)
Crystal system	monoclinic	triclinic
Space group	$P2_1/n$	$P\bar{1}$
a (Å)	14.4634(7)	7.3029(5)
b (Å)	11.0688(5)	8.2993(6)
c (Å)	15.4830(7)	9.9486(7)
α (°)	90	93.777(4)
β (°)	98.671(2)	103.920(4)
γ (°)	90	112.198(4)
V (Å^3)	2450.4(2)	533.58(7)
Z	4	1
ρ_{calc} (g/cm^3)	1.682	1.653
μ (mm^{-1})	0.785	0.702
$F(000)$	1268.0	275.0
Crystal size (mm)	0.27 × 0.23 × 0.22	0.22 × 0.20 × 0.19
Radiation	Mo Kα (λ = 0.71073)	Mo Kα (λ = 0.71073)
2Θ range for data collection (°)	4.542–51.994	5.384–59.924
Index ranges	$-17 \leqslant h \leqslant 17$, $-13 \leqslant k \leqslant 13$, $-19 \leqslant l \leqslant 19$	$-10 \leqslant h \leqslant 10$, $-11 \leqslant k \leqslant 11$, $-13 \leqslant l \leqslant 13$
Reflections collected	39520	10739
Independent reflections	4813 [R_{int} = 0.0437, R_{sigma} = 0.0262]	3049 [R_{int} = 0.0287, R_{sigma} = 0.0260]
Data/restraints/parameters	4813/0/375	3049/9/177
Goodness-of-fit (GOF) on $F2$	1.028	1.042
Final R indexes [$I \geqslant 2\sigma(I)$]	R_1 = 0.0370, wR_2 = 0.1024	R_1 = 0.0403, wR_2 = 0.1152
Final R indexes [all data]	R_1 = 0.0469, wR_2 = 0.1123	R_1 = 0.0484, wR_2 = 0.1219
Largest difference in peak and hole (e Å^{-3})	0.65 and −0.39	0.81 and −0.27

of compound **2** are presented in Table 4. The molecular graphics were prepared using MERCURY program [33].

2.4. Theoretical methods

All calculations were carried out using the TURBOMOLE version 5.9 [34] using the BP86-D3/def2-TZVP level of theory. For the calculations we have used the BP86 functional with the latest available correction for dispersion (D3) [35]. To evaluate the interactions in the solid state, we have used the crystallographic coordinates. This procedure and level of theory have been successfully used to evaluate similar interactions [36]. The theoretical study is devoted to the analysis of the supramolecular assemblies observed in the solid state of compounds **1** and **2**, giving the possibility to evaluate the different contributions to molecular recognition and to assign discrete energy values to them. The aim of the manuscript is not to find the minimum energy structure for a given complex, instead is to evaluate the binding energy of a given interaction as it is in the crystal structure. The interaction energies were computed by calculating the difference between the energies of isolated monomers and their assembly. The interaction energies were corrected for the Basis Set Superposition Error (BSSE) using the counterpoise method [37]. The molecular electrostatic potential (MEP) surfaces have been computed at the B3LYP/6-31 + G* level of theory by means of the Spartan software [38].

Table 2
Selected bond lengths (Å) and angles (°) for **1**.

Bond lengths (Å)			
Co1–O10	1.9582(16)	Co1–O20	1.9380(17)
Co1–O30	1.9626(15)	Co1–N10	1.892(2)
Co1–N20	1.890(2)	Co1–N30	1.8828(19)
Bond angles (°)			
O10–Co1–O30	96.16(7)	O20–Co1–O10	89.77(7)
O20–Co1–O30	91.20(7)	N10–Co1–O10	84.09(8)
N10–Co1–O20	173.59(8)	N10–Co1–O30	87.66(8)
N20–Co1–O10	87.48(8)	N20–Co1–O20	84.69(9)
N20–Co1–O30	174.51(8)	N20–Co1–N10	96.82(10)
N30–Co1–O10	176.39(8)	N30–Co1–O20	93.82(8)
N30–Co1–O30	84.21(7)	N30–Co1–N10	92.34(8)
N30–Co1–N20	92.41(8)	C13–O10–Co1	109.64(16)
C23–O20–Co1	109.50(16)	C33–O30–Co1	109.19(13)
O11–N10–Co1	124.43(17)	C10–N10–Co1	112.96(17)
C20–N20–Co1	112.31(17)	O31–N30–Co1	123.39(15)

Table 3
Selected bond lengths (Å) and angles (°) for **2**.

Bond lengths (Å)			
Mn1–O1W	2.2197(15)	Mn1–O1W[1]	2.2197(15)
Mn1–O2W	2.1886(12)	Mn1–O2W[1]	2.1886(12)
Mn1–O3W	2.1221(12)	Mn1–O3W[1]	2.1221(12)
O10–C13	1.2210(19)	O13–C12	1.2269(18)
O12–C11	1.2175(18)	N10–C10	1.3401(19)
O11–N10	1.2636(19)		
O11–N10–C10	119.38(13)	N11–C11–C10	116.24(12)
O1W[1]–Mn1–O1W	180.0	O2W[1]–Mn1–O1W[1]	90.73(5)
O2W[1]–Mn1–O1W	89.27(5)	O2W–Mn1–O1W	90.73(5)
O2W–Mn1–O1W[1]	89.27(5)	N10–C10–C13	125.82(14)
O2W–Mn1–O2W[1]	180.00(3)	N10–C10–C11	112.67(13)
O3W–Mn1–O1W	89.39(7)	O3W[1]–Mn1–O1W[1]	89.39(7)
O10–C13–N12	119.57(13)	O3W–Mn1–O1W[1]	90.61(7)
O3W[1]–Mn1–O1W	90.61(7)	N12–C13–C10	115.27(13)
O3W[1]–Mn1–O2W	90.11(5)	O13–C12–N12	120.18(13)
O3W–Mn1–O2W	89.89(5)	O13–C12–N11	121.47(14)
O3W[1]–Mn1–O2W[1]	89.89(5)	O3W–Mn1–O2W[1]	90.11(5)
O12–C11–N11	120.00(14)	O3W–Mn1–O3W[1]	180.0

[1] 1−x, 2−y, −z.

Table 4
Hydrogen bonds for **2**.

D	H	A	d(D-H)/Å	d(H-A)/Å	d(D-A)/Å	D-H-A/°
O1W	H1WA	O13[1]	0.838(9)	2.042(11)	2.8662(18)	168(3)
O1W	H1WB	O13[2]	0.839(9)	1.978(13)	2.7881(18)	162(2)
O2W	H2WA	O10[3]	0.849(10)	2.095(13)	2.8546(17)	149(2)
O2W	H2WB	N10[4]	0.842(9)	2.107(12)	2.8713(18)	151(2)
O3W	H3WA	O11[3]	0.847(10)	1.989(18)	2.7519(18)	149(2)
O3W	H3WB	O11[5]	0.843(9)	1.823(10)	2.6629(18)	174(3)

[1] 1 − x, 2 − y, 1 − z.
[2] −1 + x, +y, −1 + z.
[3] 1 − x, 2 − y, −z.
[4] 1 − x, 1 − y, −z.
[5] +x, 1 + y, +z.

3. Results and discussion

3.1. Synthesis and characterization

The literature reported synthesis of $[Co^{III}(DMV)_3]$ was carried out by reacting $Na_3[Co(NO_2)_6]$ with 1,3-dimethylbarbituric acid at 50 °C for 24 h [28]. However, in the present study a different synthetic route was adopted. Reaction of HDMV with $CoCl_2{\cdot}6H_2O$ in water–methanol medium and controlled pH resulted in the formation of the cobalt(III) complex $[Co^{III}(DMV)_3]{\cdot}0.5H_2O$ (**1**), also showing the aerial oxidation of precursor cobalt(II) ions. However, such oxidation (Co^{II} to Co^{III}) is not unprecedented and was previously observed with violurate as a ligand [9,27]. On the other hand, the reactivity of $MnCl_2{\cdot}4H_2O$ with HDMV in similar conditions was also explored, leading to the isolation of $[Mn^{II}(H_2O)_6](DMV)_2$ (**2**).

The IR spectra of **1** and **2** (Figs. S1 and S2 in the Supporting Information) show an expected set of bands [19,25]. For **1**, a broad band at ca. 3465 cm^{-1} is attributable to O–H stretching of water of crystallization. Three bands at *ca.* 1733, 1682 and 1636 cm^{-1} may be assigned to coupled ν(C=O) vibrations, whereas the ν(N=O) band appears at 1479 cm^{-1}. In the IR spectrum of **2**, two vibrations with maxima at 3487 and 3414 cm^{-1} are due to $\nu(H_2O)$ bands of water ligands. In addition, two weak bands at ca. 778 and 633 cm^{-1} may be assigned to the Mn-OH_2 rocking and wagging mode, respectively. For dimethylviolurate moieties, ν(C=O) bands due to two carbonyl groups appear at about 1619 and 1678 cm^{-1}. The bands at 1481 and 1288 cm^{-1} correspond to the ν(N=O) and ν(C–O) vibrations, being in agreement with the presence of anionic non-coordinated dimethylviolurate.

The cobalt(III) complex **1** is diamagnetic. The room temperature (300 K) magnetic moment of the solid **2** is 5.90 B.M. This value is in agreement with the magnetically dilute high spin d^5 Mn(II) complex [39].

3.2. Description of the crystal structures of $[Co(DMV)_3]{\cdot}0.5H_2O$ (**1**) and $[Mn(H_2O)_6](DMV)_2$ (**2**)

The structure of **1** consists of $[Co(DMV)_3]$ units and half water molecule. A perspective view of the mononuclear fragment together with the atom numbering scheme is shown in Fig. 1. In this complex, cobalt(III) atom is six-coordinated by three dimethylviolurato anions acting as bidentate ligands leading to a $[CoN_3O_3]$ chromophore in a *fac* disposition. This coordination mode has been previously observed in other metal complexes containing dimethylviolurato anions as ligands [22,40]. The coordination of each bidentate ligand forms a five-membered chelate ring, exhibiting very significant differences between the Co–N (~1.88 Å) and Co–O (~1.95 Å) distances. The coordination environment of the cobalt(III) can be considered as a slightly distorted octahedral. Half crystallization water molecule is disordered in two positions and involved in hydrogen bond with the oxygen atom O13 from the anionic ligand (2.932 Å).

The molecular structure of **2** is shown in Fig. 2. Its asymmetric unit consists of half hexaaquamanganese(II) cation and one dimethylviolurato anion (DMV). The cations are located in special positions at the inversion center. The Mn1 center is six-coordinated in a slightly distorted octahedral fashion with water molecules filling the coordination spheres. The lengths of Mn–O bonds lay between 2.1221(12) and 2.2197(15) Å, agreeing with typical values for these type of compounds [41,42]. In the crystal structure, dimethylviolurato anions are positioned forming strong H-bond interactions (2.752 and 2.855 Å) between the oxygen atoms (O11 and O10) with the O3W and O2W coordination water molecules pertaining to the hexaaquamanganese(II) cation, thus

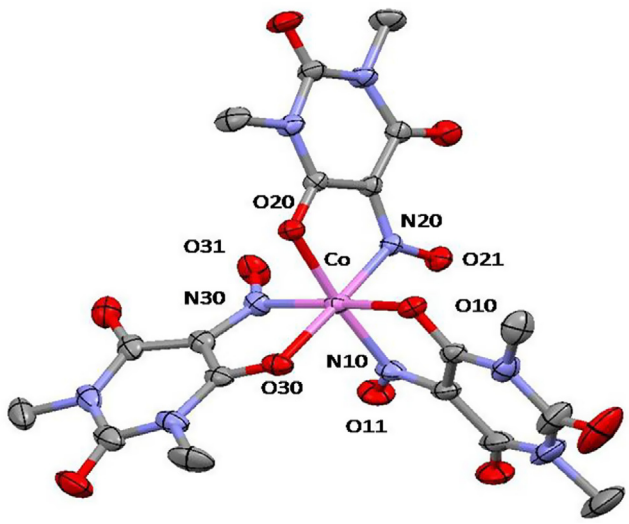

Fig. 1. Mercury perspective of the $[Co(DMV)_3]$ unit in **1**. Water molecule and hydrogen atoms are omitted for clarity; 50% probability ellipsoids are shown.

generating a trimeric unit. Further H-bonding interactions, involving also the O1W water ligands, lead to the generation of a three-dimensional supramolecular network (Fig. 3A), which is held together by several hydrogen bonds in the 2.663–2.924 Å range.

To get further insight into an intricate 3D H-bonded network in **2**, we have carried out its topological analysis by applying the concept of the simplified underlying net [43,44]. Such a net was generated by contracting $[Mn(H_2O)_6]^{2+}$ cations and $(DMV)^-$ anions to the respective centroids maintaining their connectivity via conventional hydrogen bonds [D–H···A, wherein the H···A < 2.50 Å, D···A < 3.50 Å, and ∠(D–H···A)>120°; D and A stand for donor and acceptor atoms] [43]. The obtained underling framework (Fig. 3B) can be topologically classified as a binodal 4,8-connected 3D net with the **flu** (fluorite) topology. It is defined by the point symbol of $(4^{12}.6^{12}.8^4)(4^6)_2$, wherein the $(4^{12}.6^{12}.8^4)$ and (4^6) notations correspond to the 8-connected $[Mn(H_2O)_6]^{2+}$ and 4-connected $(DMV)^-$ nodes, respectively. A few manganese coordination compounds with the present type of topology have been reported [45].

3.3. Electrochemistry

The redox properties of compounds **1** and **2** have been examined in acetonitrile and DMF solution, respectively, at GC electrode under a N_2 atmosphere; electrochemical data are summarized in Table 5. The cyclic voltammograms (CVs) of **1** and **2** (Fig. 4) show a redox couple at −0.059 and 0.532 V (versus Ag/AgCl), respectively. The peak current ratio, i_{pa}/i_{pc}, is 0.60 and 1.20 for **1** and **2**, respectively. The peaks potential differences (ΔE) of **1** and **2** are 253 and 103 mV, respectively. Since HDMV is electrochemically inert in the potential range of interest, these electrochemical processes can be assigned as metal centered. Comparison of the voltammetric peak currents with those of the ferrocene–ferrocenium couple under the same experimental conditions establishes that the redox responses in both compounds involve one electron transfer process. In general, the peak current, i_p, increases with the square root of scan rate ($\nu^{1/2}$) but does not follow in proportionality. Thus, the metal centered redox processes for compounds **1** and **2** are quasi-reversible in nature [46]. The electrochemical response for compound **1** and **2** can be ascribed to the Co^{III}/Co^{II} [47] and Mn^{II}/Mn^{III} [48] couple, respectively.

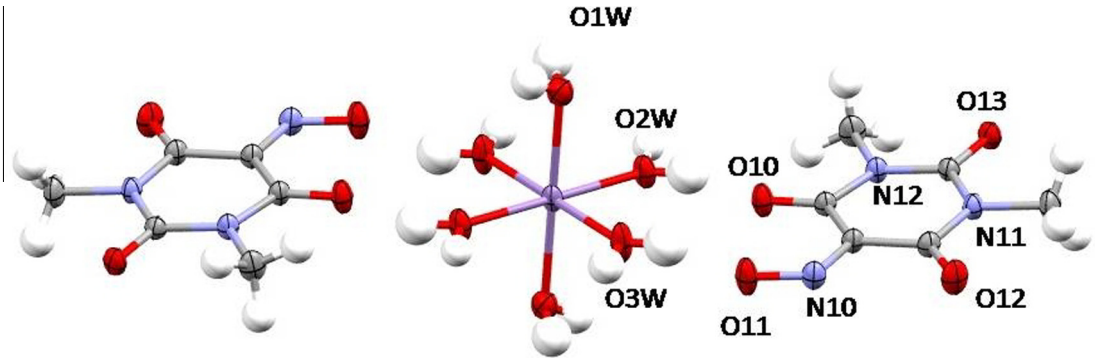

Fig. 2. Mercury perspective of **2**; 50% probability ellipsoids are shown.

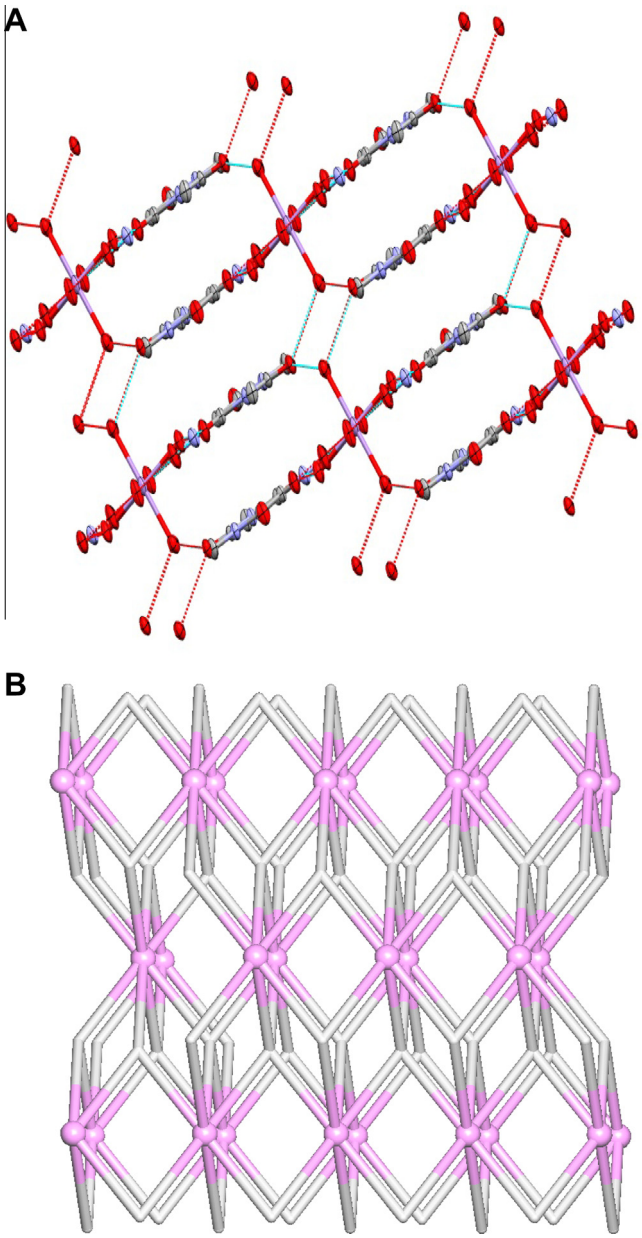

Fig. 3. Structural fragments of **2**. (A) Three-dimensional H-bonded network and (B) its topological representation showing an underlying binodal 4,8-connected net with the **flu** (fluorite) topology; (A, B) view along the *b* axis; (B) color codes: centroids of 8-connected $[Mn(H_2O)_6]^{2+}$ (magenta) and 4-connected $(DMV)^-$ (gray) nodes. (For interpretation of the references to color in this figure legend, the reader is referred to the web version of this article.)

3.4. Thermal study

To estimate the stability of **1** and **2**, thermogravimetric analyses (TGA) (Figs. S3 and S4 in the Supporting Information) were carried out between 40 and 800 °C in a static atmosphere of nitrogen. The TGA study of **1** reveals that solvent water molecule is lost below ~112 °C. After that, gradual decomposition of the desolvated sample occurs in the 165–660 °C temperature range, corresponding to the pyrolysis of dimethylviolurate molecule. The remaining residue most likely corresponds to the formation of Co_3O_4 (obsd: 13.1%; calcd: 12.9%).

Compound **2** shows a weight loss of 20.1% in the 95–155 °C interval, corresponding to the release of six coordinated water molecules (calcd: 20.3%). An anhydrous sample then decomposes in the 275–700 °C range, probably leading to the formation of MnO_2 (obsd: 16.1%; calcd: 16.4%).

3.5. Computational study

The theoretical study was focused to analyze the interesting noncovalent interactions observed in the solid state architectures of both compounds, with a special interest to the lone pair(lp)–π interactions in compound **1** and hydrogen bonding network in compound **2**. Compound **1** exhibits an intricate combination of very short lp–π contacts in the solid state that are responsible of the solid state architecture and the very compact crystal packing. A representative dimer is represented in Fig. 5A, where the dimethylviolurate ligand acts as lp donor and acceptor simultaneously. The interaction energy computed for this dimer is very large and negative ($\Delta E_1 = -30.2$ kcal/mol), being in agreement with the short lp–π distances, which is likely due to the electronic nature of the six membered ring of the ligand (π-acidity). As a matter of fact, we have represented in Fig. 5B the molecular electrostatic potential surface computed for a theoretical model of compound **1** where two dimethylviolurate ligands have been simplified. That is, the two bidentate ligands have been replaced by two 2-(hydroxyimino)acetaldehyde molecules that are also used as a O,N-bidentate ligands. This simplification not only saves computational time, it also allows a better visualization of the positive potential isosurface over the violurate ring plane in the MEP plot.

Table 5
Cyclic voltammetric data for compound **1** and **2**.

Parameter	$E_{pa}(i_{pa})$	$E_{pc}(i_{pc})$	ΔE	i_{pa}/i_{pc}	$E_{½}$
Compound **1**	0.068(9.46)	−0.185(15.68)	253	0.60	0.059
Compound **2**	0.583(18.57)	0.480(15.54)	103	1.20	0.532

E_{pa} = anodic peak potential, V; E_{pc} = cathodic peak potential, V; i_{pa} = anodic peak current, μA; i_{pc} = cathodic peak current, μA; $E_{½} = 0.5(E_{pc} + E_{pa})$ V; $\Delta E = E_{pa} - E_{pc}$, mV.

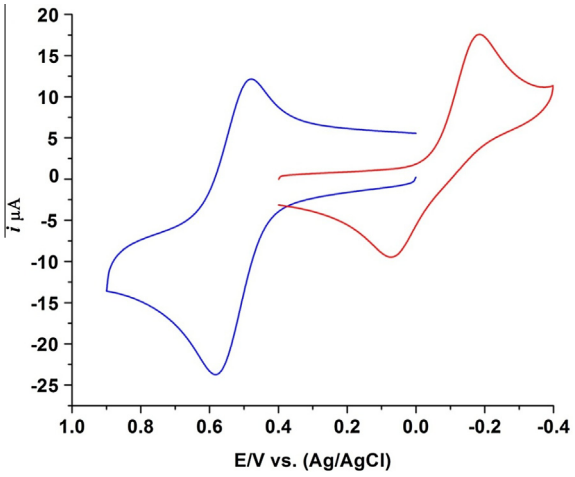

Fig. 4. Cyclic voltammogram of compound **1** in acetonitrile (red) and compound **2** in DMF (blue) at a scan rate of 100 mV s^{-1}. The concentrations of **1** and **2** were 0.893×10^{-3} and 1.011×10^{-3} M, respectively. (For interpretation of the references to color in this figure legend, the reader is referred to the web version of this article.)

If the calculation of the MEP is performed using the whole complex, the electrostatic potential over the ring does not change, thus validating the model. A small dark blue region of positive electrostatic potential over center of the ring (MEP value 20 kcal/mol) can be observed. In addition, there is a large bluish surface over the ring where the potential ranges from 14 to 18 kcal/mol. This analysis is useful to understand the compact crystal packing provoked by the network of lp–π interactions between the three dimethylviolurate ligands of the Co(III) complex, since the ligands have several lone pair donor groups and concurrently, they have a strong ability to π-interact with electron rich entities.

We have used simplified theoretical models to evaluate the lp–π interactions in compound **1** and to estimate the binding strength of the characteristic double intermolecular lp–π interaction observed between two dimethylviolurate ligands. In particular, we have used two theoretical models (see Fig. 6) based on the dimer shown in Fig. 5B and using the crystallographic coordinates. In one model (Fig. 6A), we evaluate the double lp–π interaction and an additional contribution from a C–H···O interaction involving a hydrogen atom of the methyl group and one oxygen atom (see red dashed line, Fig. 6A). As a result, the binding energy computed for this model shows that the interaction is very favorable ($\Delta E_2 = -22.7$ kcal/mol) confirming the strong ability of this ligand to participate in lp–π interactions due to coordination to the Co(III). In the second theoretical model (Fig. 6B), we have substituted one dimethylviourate ligand by violurate in the Co(III) complex with the purpose to eliminate this hydrogen bonding contribution. As a result, the interaction energy is slightly reduced to $\Delta E_3 = -21.7$ kcal/mol, indicating that the contribution of this hydrogen bond is very small, which agrees with the long distance (2.82 Å) and small C–H···O angle (97.2°).

The formation of strong hydrogen bonds by coordinated water molecules is a topic of recent interest [49]. In the theoretical study of compound **2** we have focused our attention to evaluate the hydrogen bonding network that is observed in the crystal packing. This hydrogen bonding network generates interesting supramolecular assemblies in the solid state where the equatorial water molecules of the $[Mn(H_2O)_6]^{2+}$ moiety act as strong hydrogen bonding donors and the dimethylviourate molecules as hydrogen bonding acceptors. Two different binding modes are observed in the formation of the pentameric assembly where one central $[Mn(H_2O)_6]^{2+}$ moiety interacts with four coplanar dimethylviolurate rings (see Fig. 7A). Starting from two different trimeric units (formed by one $[Mn(H_2O)_6]^{2+}$ and two dimethylviolurates), we have analyzed the energetic features of both binding modes. We have started from these trimers because they are neutral and the strong and non-directional electrostatic effects are minimized. In both binding modes three H-bonds are formed, see green and blue dashed lines in Fig. 7. In the first one, both atoms of the N–O bond participate in the formation of two hydrogen bonds and the other one is formed with one C=O group of the ring (blue lines). The interaction energy that corresponds to these three H-bonds is

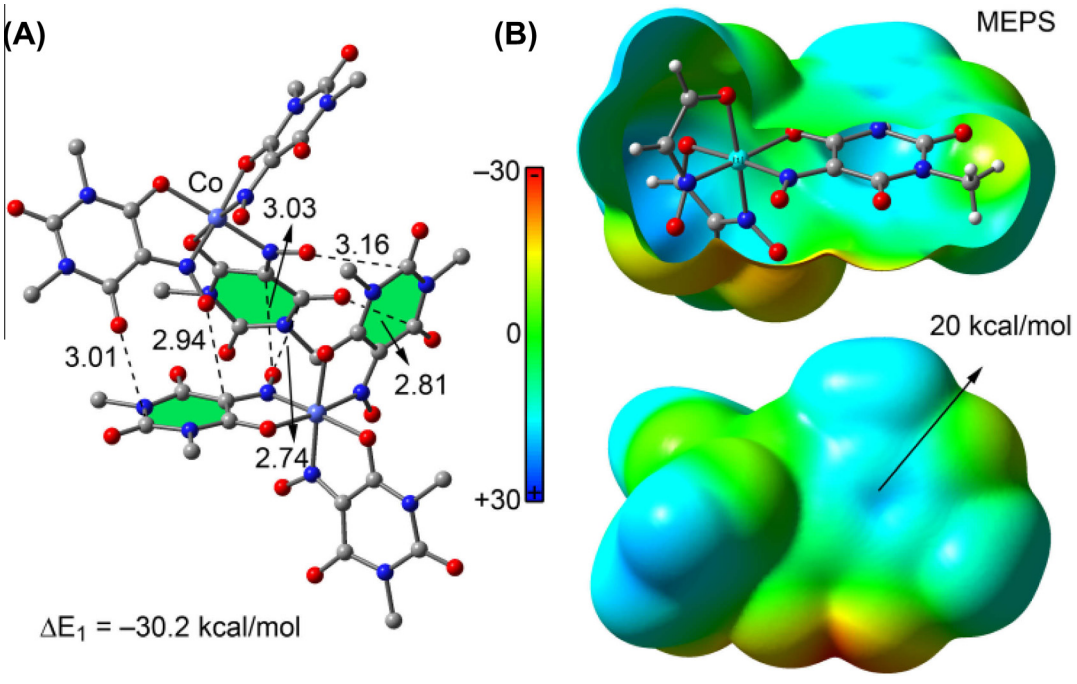

Fig. 5. Dimer of compound **1** (A) and MEP surfaces of a model of **1** (B). Distances in Å (left). Hydrogen atoms have been omitted for the sake of clarity.

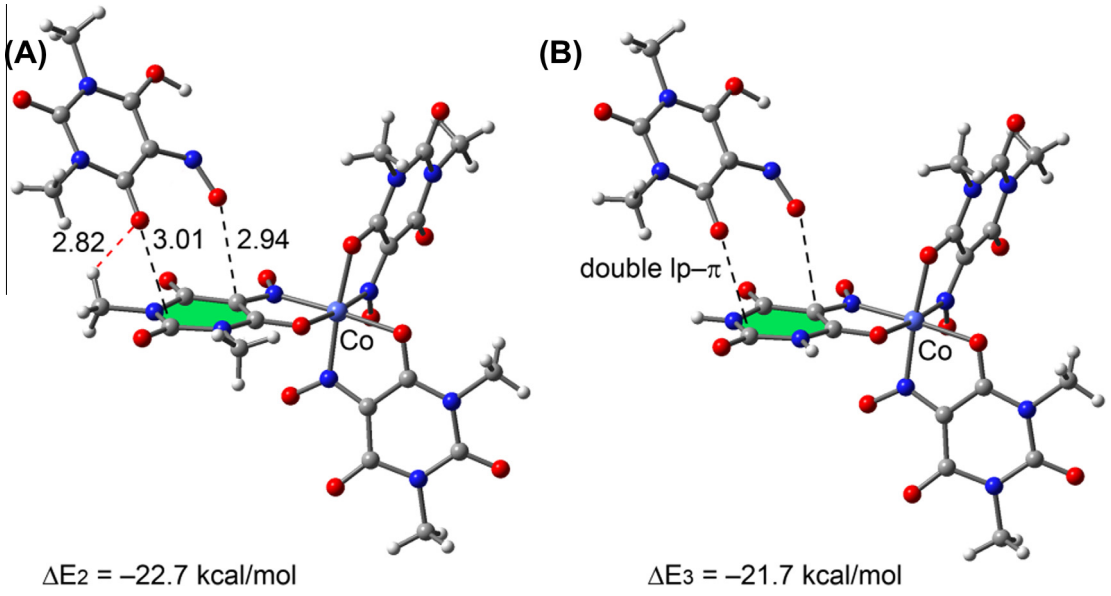

Fig. 6. Theoretical models used to evaluate the double lp–π interaction in compound **1**. Distances in Å.

½ × ΔE_4 = −20.5 kcal/mol. In the second binding mode (green lines), one C═O group forms a bifurcated hydrogen bond and the exocyclic N–O group also establishes an N–O···H bond. This binding mode is considerably more favorable ½ × ΔE_5 = −33.5 kcal/mol than the other one, in agreement with the shorter distances. In addition to these two binding modes that are responsible for the formation of the supramolecular assembly in the solid state of **2**, the apical water molecules also participate in H-bonding interactions as connectors of supramolecular assemblies (see Fig. 7B). We have also evaluated the interaction energy of this complex that

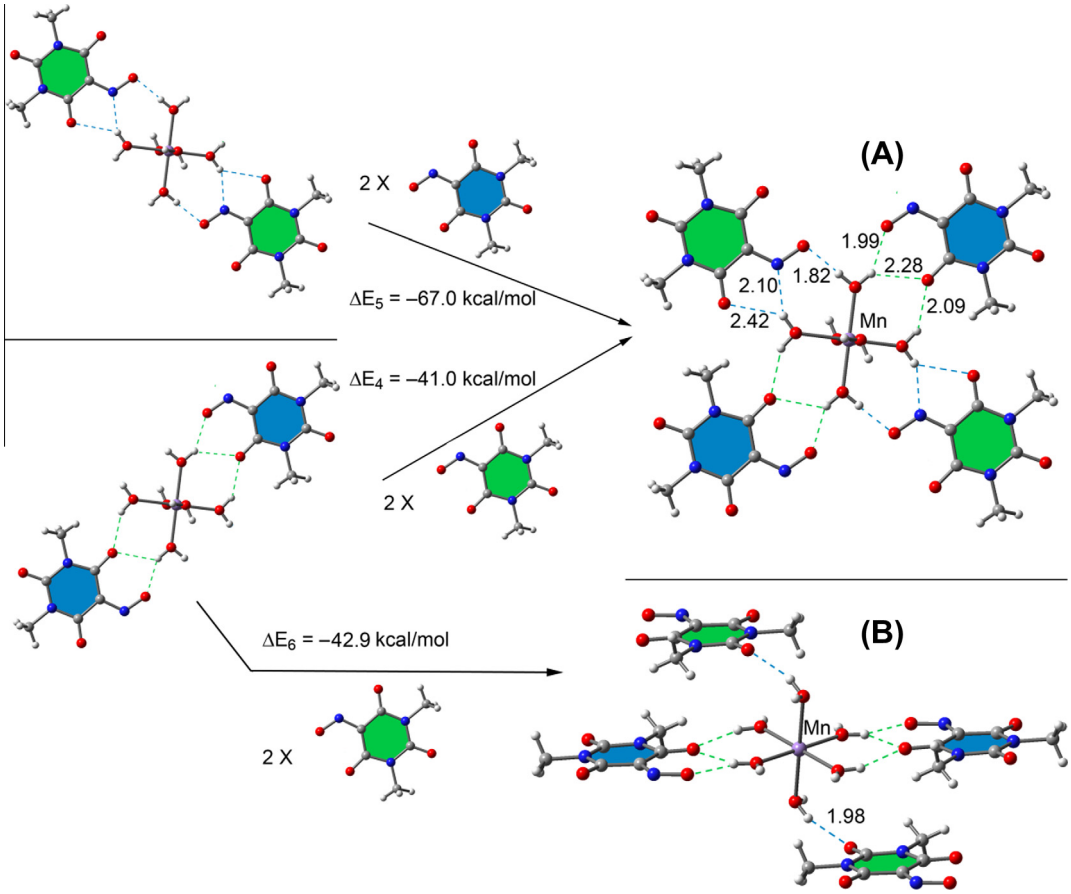

Fig. 7. Partial view of the crystal packing of compound **2** with indication of the different noncovalent interactions. The equations used to evaluate the energetic contributions are also shown. Distances in Å.

is $\Delta E_6 = -42.9$ kcal/mol, therefore each hydrogen bonding contributes in $\frac{1}{2} \times \Delta E_6 = -21.5$ kcal/mol. The interaction energies of the hydrogen bonds are very large in absolute value due to the anionic nature of the hydrogen bond acceptor and the strong acidity of the hydrogen bond donor (Mn-coordinated water molecules).

4. Conclusion

In the present work, the variation of role of HDMV (*N*,*N*′-dimethylvioluric acid monohydrate) as ligand or counteranion on Co(III) and Mn(II) ions has been investigated. Accordingly, two Co(III) and Mn(II) compounds have been synthesized and characterized by IR spectroscopy, X-ray crystallography, TGA and electrochemical study. The solid state architecture of **1** is completely dominated by the formation of multiple and strong lp–π interactions. In contrast, the presence of the $[Mn(H_2O)_6]^{2+}$ moiety provokes the generation of an intricate 3D hydrogen bonding network in the structure of **2**. This network has been topologically classified as a binodal 4,8-connected net with the **flu** (fluorite) topology. Hence, the present study also contributed to the topological classification of complex supramolecular networks. By the DFT study of compound **1**, we have analyzed the molecular electrostatic potential surface and found that the coordinated dimethylviolurate ring has a strong ability to interact with electron rich groups. In compound **2**, we have analyzed the different binding modes that contribute to the formation of the supramolecular assembly in the solid state. The contributions of the different binding forces have been evaluated using several models that confirm the importance of both lp–π and H-bonding interactions.

Acknowledgements

Financial assistance from Department of Biotechnology, Government of India [vide sanction No BCIL/NER-BPMC/2012.1549] is gratefully acknowledged. One of the authors, R.B. is grateful to the authority of NIT-Agartala for providing Institute fellowship. We thank SAIF, Department of Instrumentation & USIC, Gauhati University, for single crystal X-ray diffraction data. A.B. and A.F. thank DGICYT of Spain (project CONSOLIDER INGENIO CSD2010-00065, FEDER funds) for funding. We also thank the CTI (UIB) for free allocation of computer time. We acknowledge the anonymous reviewers whose comments and suggestions were helpful during the revision process.

Appendix A. Supplementary material

CCDC 1047263 and 1047274 contain the supplementary crystallographic data for (**1**) and (**2**). These data can be obtained free of charge from The Cambridge Crystallographic Data Centre via www.ccdc.cam.ac.uk/data_request/cif. Supplementary data associated with this article can be found, in the online version, at http://dx.doi.org/10.1016/j.ica.2015.06.018.

References

[1] S.J. Langford, J.S. Stoddart, Pure Appl. Chem. 68 (1996) 1255.
[2] (a) J.S. Lindsey, New J. Chem. 15 (1991) 153;
(b) D. Philp, J.F. Stoddart, Angew. Chem., Int. Ed. Engl. 35 (1996) 1154;
(c) G.M. Whitesides, B. Grzybowski, Science 295 (2002) 2418.
[3] W. Muller, H. Ringsdorf, E. Rump, G. Wildburg, X. Zhang, L. Angermaier, W. Knoll, M. Liley, J. Spinke, Science 262 (1993) 1706.
[4] (a) J. Rebek Jr., Chem. Br. 30 (1994) 286;
(b) T. Li, K.C. Nicolaou, Nature 396 (1994) 218;
(c) D. Sievers, G. von Kiedrowski, Nature 369 (1994) 221;
(d) F.M. Menger, A.V. Eliseev, N.A. Khanjin, J. Am. Chem. Soc. 116 (1994) 3613.
[5] R. Chakrabarty, P.S. Mukherjee, P.J. Stang, Chem. Rev. 111 (2011) 6810.
[6] (a) S.T. Nguyen, D.L. Gin, J.T. Hupp, X. Zhang, Proc. Natl. Acad. Sci. 98 (2001) (1850) 11849;
(b) H. Xu, X. Zhang, J. Sun, S. Cui, Supramolecular Chemistry: from molecular architecture to functional assemblies, Encyclopedia of Life Support System, 2010.
[7] K.T. Mahmudov, M.N. Kopylovich, A.M. Maharramov, M.M. Kurbanova, A.V. Gurbanov, A.J.L. Pombeiro, Coord. Chem. Rev. 265 (2014) 1.
[8] (a) G.S. Nichol, W. Clegg, Acta Crystallogr., Part C 61 (2005) o721;
(b) K. Guille, R.W. Harrington, W. Clegg, Acta Crystallogr., Part C 63 (2007) o327.
[9] J. Moratal, J. Faus, Inorg. Chim. Acta 25 (1977) L1.
[10] (a) R.W. Awadallah, M.K. Sheriff, A.A.M. Gad, J. Ind. Chem. Soc. 59 (1984) 624;
(b) M. Kavlakova, A. Bakalova, G. Momekov, D. Ivanov, Arzneimittelforschung 62 (2012) 599;
(c) N.A. Illán-Cabeza, A.R. García-García, J.M. Martínez-Martos, M.J. Ramírez-Expósito, M.N. Moreno-Carretero, J. Inorg. Biochem. 126 (2013) 118;
(d) N.A. Illán-Cabeza, S.B. Jiménez-Pulido, M.J. Ramírez-Expósito, A.R. García-García, T. Peña-Ruiz, J.M. Martínez-Martos, M.N. Moreno-Carretero, J. Inorg. Biochem. 143 (2015) 20.
[11] (a) M. Husain, Q. Husain, Crit. Rev. Environ. Sci. Technol. 38 (2008) 1;
(b) E. Quintana, C. Valls, T. Vidal, M. Blanca, Bioresour. Technol. 148 (2013) 1.
[12] F. Abraham, A. Nowogrocki, G.S. Sueur, C. Bremard, Acta Crystallogr., Part B 38 (1980) 799.
[13] M. Hamelin, Acta Crystallogr., Part B 28 (1972) 228.
[14] K. Tamaki, N. Okabe, Acta Crystallogr., Part C 52 (1996) 1125.
[15] J. Faus, F. Lloret, M. Julve, J.M. Clemente-Juan, M.C. Munoz, X. Solans, M. Font-Bardia, Angew. Chem. 35 (1996) 1485.
[16] H. Gillier, Bull. Soc. Chim. (1965) 2373.
[17] M. Hamelin, Acta Crystallogr., Part B 32 (1976) 364.
[18] H.C. Garcia, R. Diniz, N.L. Speziali, L.F.C. de Oliveira, J. Mol. Struct. 1070 (2014) 117.
[19] N.A. Illán-Cabeza, A.R. García-García, M.N. Moreno-Carretero, Inorg. Chim. Acta 366 (2011) 262.
[20] M.A.R. Molina, J.D.M. Ramos, J.D.D.L. Gonzalez, C.V. Calahorro, An. Quim. 79 (1983) 200–206.
[21] C. Ruiz-Valero, A. Monge, E. Gutierrez-Puebla, E. Gutierrez-Rios, Acta Crystallogr., Part C 40 (1984) 811.
[22] M.A. Romero, J.M. Salas, M. Simard, M. Quiros, A.L. Beauchamp, Polyhedron 9 (1990) 2733.
[23] J. Faus, M. Julve, F. Lloret, J.A. Real, J. Sletten, Inorg. Chem. 33 (1994) 5535.
[24] E. Colacio, C. Lopez-Magana, V. McKee, A. Romerosa, J. Chem. Soc., Dalton Trans. (1999) 2923–2926.
[25] R. Banik, S. Roy, A. Bauza, A. Frontera, S. Das, RSC Adv. 5 (2015) 10826.
[26] K. Tamaki, N. Okabe, Acta Crystallogr., Part C 52 (1996) 1124.
[27] Z.-J. Xiao, S.-X. Liu, Chin. J. Struct. Chem. 25 (2006) 163.
[28] C. Bremard, G. Nowogrocki, S. Sueur, J. Chem. Soc., Dalton Trans. (1981) 1856.
[29] SAINT, Data Reduction and Frame Integration Program for the CCD Area-Detector System. Bruker Analytical X-ray Systems, Madison, Wisconsin, USA, 1997–2006.
[30] G.M. Sheldrick, SADABS, Program for Area Detector Adsorption Correction, Institute for Inorganic Chemistry, University of Göttingen, Germany, 1996.
[31] L.J. Bourhis, O.V. Dolomanov, R.J. Gildea, J.A.K. Howard, H. Puschmann, Acta Crystallogr., Part A 71 (2015) 59.
[32] G.M. Sheldrick, Acta Crystallogr., Part A 64 (2008) 112.
[33] C.F. Macrae, I.J. Bruno, J.A. Chisholm, P.R. Edgington, P. McCabe, E. Pidcock, L. Rodriguez-Monge, R. Taylor, J. van de Streek, P.A. Wood, Mercury CSD 2.0, J. Appl. Crystallogr. 41 (2008) 466–470.
[34] R. Ahlrichs, M. Bär, M. Hacer, H. Horn, C. Kömel, Chem. Phys. Lett. 162 (1989) 165.
[35] S. Grimme, J. Antony, S. Ehrlich, H. Krieg, J. Chem. Phys. 132 (2010) 154104.
[36] (a) A. Bauzá, A. Terrón, M. Barceló-Oliver, A. García-Raso, A. Frontera, Inorg. Chim. Acta 2015 (2015), http://dx.doi.org/10.1016/j.ica.2015.04.028;
(b) D. Sadhukhan, M. Maiti, G. Pilet, A. Bauzá, A. Frontera, S. Mitra, Eur. J. Inorg. Chem. 11 (2015) 1958;
(c) M. Mirzaei, H. Eshtiagh-Hosseini, Z. Bolouri, Z. Rahmati, A. Esmaeilzadeh, A. Hassanpoor, A. Bauza, P. Ballester, M. Barceló-Oliver, J.T. Mague, B. Notash, A. Frontera, Cryst. Growth Des. 15 (2015) 1351;
(d) P. Chakraborty, S. Purkait, S. Mondal, A. Bauzá, A. Frontera, C. Massera, D. Das, CrystEngComm 17 (2015) 4680.
[37] S.F. Boys, F. Bernardi, Mol. Phys. 19 (1970) 553.
[38] Spartan' 10, v. 1.10, Wavefunction Inc., Irvin, CA, USA.
[39] G. Batra, P. Mathur, Transition Met. Chem. 19 (1994) 160.
[40] F. Almazán, E. García-España, M. Mollar, F.L. Loret, M. Julve, J. Faus, J. Chem. Soc., Dalton Trans. (1990) 2565.
[41] C.R. Maldonado, M. Quirós, J.M. Salas, A. Rodríguez-Diéguez, Inorg. Chim. Acta 362 (2009) 1553.
[42] L.-H. Huo, S. Gao, S.W. Ng, Acta Crystallogr. E65 (2009) m1504.
[43] (a) V.A. Blatov, IUCr CompComm Newslett. 7 (2006) 4;
(b) V.A. Blatov, A.P. Shevchenko, D.M. Proserpio, Cryst. Growth Des. 14 (2014) 3576.
[44] (a) M. O'Keeffe, O.M. Yaghi, Chem. Rev. 112 (2012) 675;
(b) M. Li, D. Li, M. O'Keeffe, O.M. Yaghi, Chem. Rev. 114 (2014) 1343.
[45] (a) J. Tian, L.V. Saraf, B. Schwenzer, S.M. Taylor, E.K. Brechin, J. Liu, S.J. Dalgarno, P.K. Thallapally, J. Am. Chem. Soc. 134 (2012) 9581;
(b) T.-F. Liu, J. Lü, C. Tian, M. Cao, Z. Lin, R. Cao, Inorg. Chem. 50 (2011) 2264;
(c) M.-H. Xie, X.-L. Yang, C.-D. Wu, Chem. Eur. J. 17 (2011) 11424.
[46] R. Greef, R. Peat, L.M. Peter, D. Pletcher, J. Robinson, Instrumental Methods in Electrochemistry, Ellis Horwood Ltd., England, 1985. p. 188.

[47] (a) A. Böttcher, T. Takeuchi, K.I. Hardcastle, T.J. Meade, H.B. Gray, Inorg. Chem. 36 (1997) 2498;
(b) E.S. Wiedner, J.A.S. Roberts, W.G. Dougherty, W.S. Kassel, D.L. DuBois, R.M. Bullock, Inorg. Chem. 52 (2013) 9975;
(c) H. Ogino, K. Ogino, Inorg. Chem. 22 (1983) 2208.
[48] (a) S.J. Brudenell, L. Spiccia, A.M. Bond, G.D. Fallon, D.C.R. Hockless, G. Lazarev, P.J. Mahon, E.R.T. Tiekink, Inorg. Chem. 39 (2000) 881;
(b) W. Shuangxi, Z. Ying, Z. Fangjie, W. Qiuying, W. Liufang, Polyhedron 11 (1992) 1909;
(c) D. Sivanesan, S. Kannan, T.D. Thangadurai, K.-D. Jung, S. Yoon, Dalton Trans. 43 (2014) 11465.
[49] (a) J.M. Andrić, G.V. Janjić, D.B. Ninković, S.D. Zarić, Phys. Chem. Chem. Phys. 14 (2012) 10896;
(b) D.Z. Vojislavljević, G.V. Janjić, D.B. Ninković, A. Kaporc, S.D. Zarić, CrystEngComm 15 (2013) 2099;
(c) C. Husberg, U. Ryde, J. Biol. Inorg. Chem. 18 (2013) 499.